Photoionization Cross Section of Neon in the 80 to 600 Å Region*

D. L. EDERER AND D. H. TOMBOULIAN

Laboratory of Atomic and Solid State Physics, Cornell University, Ithaca, New York

(Received 28 October 1963)

The paper presents measurements of the absolute photoionization cross section of neon in the soft x-ray region (80–600 Å) to an accuracy of 5% or better. Increased reliability of measurements has been brought about by various technical improvements such as the use of an absorber cell with suitable windows and the use of a Geiger-Mueller tube specially designed for counting photons whose energy was in excess of 40 eV. At the $L_{2,3}$ threshold (575 Å) the cross section σ has a value of 6.3 Mb, rises to a peak value of 10.0 Mb at 375 Å, and then decreases to 7.8 Mb at the L_1 edge (about 261 Å). The range of measurements has been extended to 10 Ry above the ionization threshold. Consequently, it has been possible to join the results with previous observations made at high energies. With the exception of He, neon is the only other gas for which the value of σ is known over a large energy range with sufficient precision. This information, combined with estimates of discrete oscillator strengths, has led to the first successful evaluation of the Thomas-Reiche-Kuhn sum rule.

I. INTRODUCTION

IT is the purpose of this paper to present measurements on the photoionization cross section of neon in the spectral range extending from 80 to 600 Å. The photoionization cross section of this rare-gas atom has also been investigated experimentally by Po Lee and Weissler[1] and also by Ditchburn.[2]

The research was undertaken with a view to (1) extend the range of available data and (2) to improve the existing measurements by adopting more refined procedures developed in this laboratory in connection with the investigation on the photoionization of helium. The technique referred to consists in confining the gas sample to a cell with sufficiently transparent windows. The use of a cell reduces the likelihood of contamination and facilitates the determination of gas pressures. An additional refinement in the procedure was to use a GM (Geiger-Mueller) counter as a detector of radiation below 300 Å. Over the region of overlap, the results obtained from conventional photometric measurements could then be compared with those obtained by the photon counting scheme. Such a comparison adds to the reliability of the measurements.

Experimentally, the total cross section σ_T is measured by observing the intensity change suffered by a beam of photons after it passes through the volume of a gas whose concentration is N atoms/cc. In the wavelength region of interest σ_T is assumed equal to the photoionization cross section σ. This is not inconsistent with investigation of the photoionization process in rare gases.[3,4] Other scattering cross sections (Compton and Thompson) are smaller by many orders of magni-

tude. The cross section is given by the usual relation

$$\sigma = (760/p)(T/273)(1/N_0 x)[\ln(I(o)/I(p))], \quad (1)$$

where $I(o)$ is the intensity of the incident beam, $I(p)$ the intensity transmitted by a column of gas, x cm in length, p the gas pressure in Torr, T the absolute temperature, and N_0 is 2.69×10^{19} per cc.

The $I(o)/I(p)$ ratio may also be arrived at by measuring the ion current produced by a known photon flux. This is an inherently more difficult approach since it involves the measurement of absolute fluxes and of small ion currents. The latter method must be used in determining the photoionization cross section of molecules where the absorption of a photon may lead to processes other than photoionization.

II. EXPERIMENTAL

Observations extending from 225 Å to the $L_{2,3}$ edge at 575 Å were obtained by the use of a normal incidence vacuum spectrograph equipped with photographic detection. Measurements below 225 Å were carried out on two different grazing incidence spectrographs. One was equipped to record photon fluxes photographically while in the other instrument, a GM counter, was used to detect photons. Many features descriptive of instrumental arrangements are to be found in a previous paper.[5] A discussion of certain aspects of particular importance to the work with neon is included.

A. Gas Cell

A schematic diagram of a typical cell is shown in Fig. 1. The thickness of the cell was approximately 1.0 cm and its diameter ranged from 1.6 to 1.9 cm. In the photographic method the cell was located directly behind the entrance slit, while in the measurements with the GM counter, it was placed in front of the analyzing slit of the counter. In making absorption measurements, the windows constitute a critical component in the

* Research supported by the U. S. Office of Naval Research.
[1] Po Lee and G. L. Weissler, Proc. Roy. Soc. (London) 220A, 71 (1953).
[2] R. W. Ditchburn, Proc. Phys. Soc. (London) A76, 461 (1960).
[3] N. Wainfan, W. C. Walker, and G. L. Weissler, Phys. Rev. 99, 542 (1955).
[4] P. H. Metzger and G. R. Cook, Bull. Am. Phys. Soc. 8, 476 (1963).

[5] D. J. Baker, D. E. Bedo, and D. H. Tomboulian, Phys. Rev. 124, 1471 (1961).
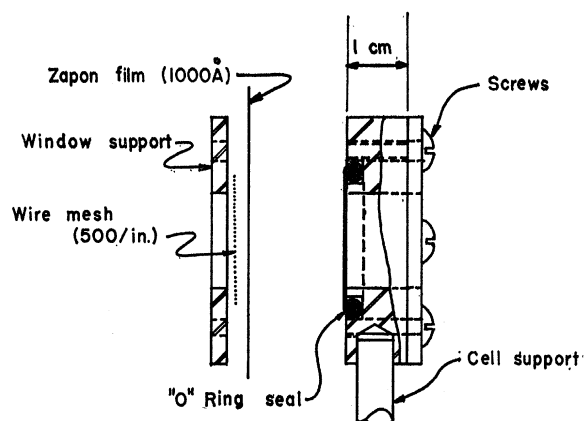
FIG. 1. A schematic diagram which shows the constructional features of a typical gas cell. The left-hand portion represents window structure and the assembled cell is shown at the right.

construction of the cell and of the counter. A fine mesh (~500/in.) is cemented to the stainless steel window form. A film of Zapon, about 500 Å in thickness, is picked up with a wire hoop and placed over the window frame. To minimize the possibility of leaks and to withstand higher pressures, two layers of plastic were used. Double thickness windows are especially needed in the case of GM counters where the operating pressure of the gas may be as high as 120 Torr.

At wavelengths in excess of 400 Å, Zapon films become highly absorbing and one must resort to the use of single-layer windows. Such windows were subject to slight leaks. However, this defect did not render them useless provided one took account of changes in the source caused by the leak.

In the long wavelength region (200–700 Å) the beam attenuation per window was between 25 and 50, while around 100 Å the corresponding quantity was only about 5. In each case, the wire screens alone gave rise to an attenuation of 3.

The concentration of impurities in the gas sample ranged from 20 ppm for He to less than 4 ppm for N_2, O_2, and Ar. Contaminants at such concentrations do not affect the measurements. The gas pressure was measured by an aneroid gauge calibrated against mercury and oil manometers. The three devices gave consistent results. The pressures ranged between 2 and 15 Torr with an uncertainty of ± 0.15 Torr.

B. Measurements with GM Counters

Until recently, the use of GM counters in the measurement of photon fluxes in the soft x-ray region[6] has been limited to photon energies in excess of 100 eV. It has been shown[7] that lower energy photons may also be detected by its use. The behavior of the GM counter

in recording absolute fluxes at wavelengths longer than 100 Å will be described elsewhere.[8]

The counting technique is advantageous because it enables one to test the stability of sources, and to measure hundred-fold attenuations introduced by the gas—a task well nigh impossible photometrically. The particular detector was also found to be a suitable tool in studying the effect of leaky windows by measuring the cross section with a thin (leaky) and thick (leak proof) window.

C. Procedural

In the course of the absorption measurements, several types of sources were used. These included: (1) line sources produced by condensed discharges through a capillary or by a gas discharge in a Penning tube[9]; (2) the characteristic $L_{2,3}$ Al emission band (edge at 170 Å). In the long-wavelength region, where the gas absorption is high, exposures were made with a spark source and a normal incidence spectrograph. The exposures ranged from about 10 sparks with no windows or gas in the beam to several thousand sparks when the gas cell was introduced. The spark ratio between exposures taken with gas and without gas in the cell ranged between 2 and 4. The photometric reductions were carried out by procedures described previously.[10] In generating the calibration curve of the special emulsions (Eastman SWR, Ilford QI) the method of Woodruff and Givens[11] was followed.

With a fresh Al target, the counting rate of the GM counter at $\lambda = 180$ Å was about 20 000 per min when the anode of the x-ray tube was operated at a voltage of 1.8 kV and a current of 110 mA. Under typical operating conditions the pressure of the counting gas (helium-isobutane mixture) was kept at about 60 Torr to within 1%. At this pressure the anode voltage was maintained at 1000 V and the counter characteristic had a plateau 100 V wide. The radiation incident on the counter was analyzed by a 10-mil slit, mounted on the counter. A 6000-Å Al foil was inserted in the beam to filter out short-wavelength radiations which would otherwise fall on the counter in the second or third order. Such a filter had an attenuation of 5 at 180 Å just above the $L_{2,3}$ edge, while its attenuation at 90 and 60 Å was calculated to be about 1000 and 100, respectively. When using the Penning discharge, typical counting rates were around 5000 per min for the stronger lines of helium and neon. This source has a low continuous background, and no filters were needed to remove order contamination.

To safeguard against errors which may arise from slow time variations in the incident intensity, the measurement of $I(p)$ was alternated with that of $I(o)$.

[6] A. P. Lukirskii, M. A. Ramak, and L. A. Smirnov, Opt. i Spektroskopiya 9, 505 (1960) [English transl.: Opt. Sectry. (USSR) 9, 262 (1960)].

[7] D. L. Ederer and D. H. Tomboulian, J. Opt. Soc. Am. 52, 1312 (1962).

[8] D. L. Ederer and D. H. Tomboulian (to be published).

[9] R. D. Deslattes, T. J. Peterson, and D. H. Tomboulian, J. Opt. Soc. Am. 53, 302 (1963).

[10] D. H. Tomboulian, Handbuch der Physik, edited by S. Flügge (Springer-Verlag, Berlin, 1957), Vol. 30, p. 246.

[11] R. W. Woodruff and M. P. Givens, Phys. Rev. 97, 52 (1955).

The value of $I(o)$ at the midpoint of the interval be-tween two successive determinations of $I(o)$ was assumed to represent the incident flux to be associated with a given counter measurement of $I(p)$.

III. TREATMENT OF DATA AND RESULTS

The photographic scheme gives the attenuation as a function of wavelength at a fixed pressure, while the counter measurements yield the attenuation as a function of pressure at a fixed wavelength. In the photometric approach, the attenuation $I(o)/I(p)$ is obtained by comparing line intensities with and without gas in the cell. The cross section at a given wavelength is then computed with the aid of Eq. (1). The cross sections deduced from various runs were averaged.

After correcting the counting rates for dead time and background, $\ln(I(o)/I(p))$ was plotted as a function of p. The cross section σ was obtained from the counter measurements at various wavelengths by fitting the best straight lines to such plots and evaluating its slope which is proportional to σ. Figure 2 includes a plot of this sort for two different wavelengths. A departure from linearity would imply[12] that the absorption law is invalid or that the physical dimensions of the cell were subject to change with pressure. A failure of the absorption law for a rare gas at the low pressures is not expected. Hence a departure from a straight line is to be ascribed to changes in the cell (pressure dependence of window thickness and the path length).

The average value of the cross section as a function of the photon wavelength and energy is presented in Table I. The measurements denoted by an asterisk were obtained by the use of GM counters. The errors in these measurements range from ± 0.2 to ± 0.4 Mb. The number of photometric observations at each photon energy are also shown in the same column. Since the data represent absolute values of the cross section, consideration was given to the elimination of systematic errors. Such errors in the attenuation ratio may arise from (1) fluctuations in the source intensity, and (2) order contamination and errors inherent in the detectors. In using the spark source, fluctuations were minimized by random mixing of exposures. In the case of steady current sources (x-ray targets and gas discharges) the emission was monitored in time and corrections were made as described. Short-wavelength radiation appearing in higher orders alters the attenuation significantly. Only known first-order lines were utilized and appropriate filters were provided when making measurements with counters. The fractional error due to counting statistics was less than 4%. However, the average mean-square deviation of the cross section for each wavelength was found to change by a factor of two from the most to the least precise

[12] R. W. Ditchburn and U. Opik, in *Atomic and Molecular Processes*, edited by D. R. Bates (Academic Press Inc., New York, 1962).
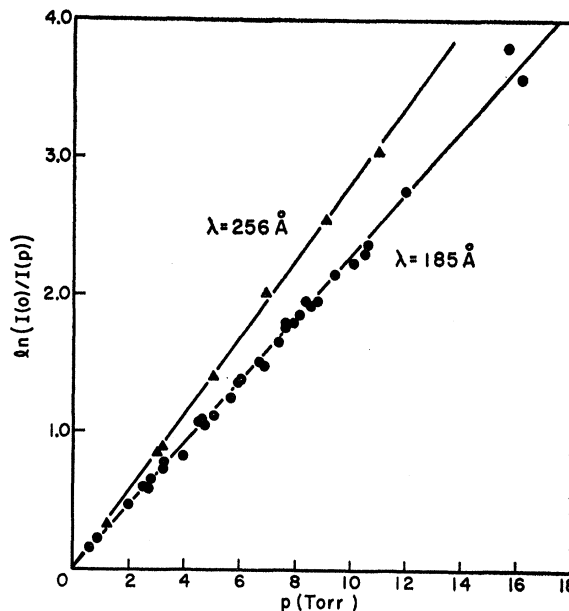

FIG. 2. A plot of $\ln(I(o)/I(p))$ as a function of pressure for two wavelengths.

measurements. In making a comparison of the radiant power at a fixed wavelength, by the use of an emulsion, the scatter of points is minimum if only the linear portion of the calibration curve is utilized. Even if all the conventional precautions are observed in the processing of the emulsion, there still remains the effect of varying sensitivity of the emulsion from one portion to another.

The strongest argument for confidence in the data lies in the agreement between photometric and counter measurements, after the removal of systematic errors which are common to both schemes of detection. It is gratifying that observations of the cross section made with a variety of sources and entirely different detectors are free from discrepancies.

Next we consider the measurement of the remaining quantities T, p, and x necessary for the evaluation of the cross section. Owing to the expansion of the gas as the latter passes from the reservoir to the cell, for neon (a real gas) one expects a temperature change of one degree centigrade corresponding to a pressure drop of about one atmosphere. One therefore is justified in assuming that the process is isothermal and the temperature of the gas in the cell was taken to be the same as that of the room.

The pressure determination could be carried out to within ± 0.15 Torr, but the measurement was made not at the cell but at a distance of about 20 cm from it. In the absence of a leak in the cell, such a determination did yield the cell pressure correctly. However, there was no observable change in the attenuation even when the cell window was known to have a small leak. Hence, it was concluded that a negligible pressure gradient did exist between the point of observation and the cell.

D. L. EDERER AND D. H. TOMBOULIAN

TABLE I. Absolute photoionization cross section of neon. Columns 1 and 2 contain, respectively, the wavelength in Å and energy of the incident photon in Ry. Observations denoted by an asterisk were made by the use of GM counters.

| Wavelength in Å	Photon energy in Ry	No. and type of obs.	σ in Mb	Wavelength in Å	Photon energy in Ry	No. and type of obs.	σ in Mb
80.57	11.31	5	2.49	260.4	3.50	6	8.74
83.50	10.92	6	2.52	263.4	3.46	1.	8.80
83.52	10.68	6	2.75	267.0	3.41	3	8.52
90.40	10.08	5	3.01	267.5	3.41	*	7.85
96.58	9.44	6	2.64	277.3	3.29	1	7.65
99.60	9.14	6	2.88	283.5	3.22	*	8.00
104.8	8.70	6	3.38	283.3	3.22	2	7.99
110.5	8.25	6	3.72	285.8	3.19	4	8.33
115.8	7.87	5	3.70	294.5	3.09	1	8.78
117.8	7.73	5	3.79	295.7	3.08	5	8.84
119.0	7.66	7	3.88	299.8	3.04	4	8.66
129.8	7.02	6	4.40	301.1	3.03	*	9.03
133.4	6.84	6	4.71	303.6	3.00	5	9.08
135.5	6.73	6	4.78	303.6	3.00	*	9.00
138.0	6.60	5	4.95	305.8	2.98	5	9.22
150.0	6.07	3	5.65	306.8	2.97	5	9.11
151.5	6.02	6	5.62	308.2	2.96	1	9.00
159.4	5.72	7	5.96	311.8	2.93	5	9.08
162.5	5.61	4	6.09	321.0	2.85	2	8.97
164.6	5.54	7	6.08	328.4	2.77	2	9.44
166.2	5.49	4	6.23	355.3	2.56	3	10.08
168.1	5.42	5	6.30	359.2	2.54	4	10.16
172.2	5.29	5	6.58	364.7	2.50	1	9.59
173.0	5.27	6	6.78	374.2	2.44	4	10.16
184.0	4.95	5	6.76	378.1	2.40	1	9.34
185±0.5	4.93	*	6.92	379.7	2.40	4	9.97
185.7	4.91	5	7.10	384.1	2.38	4	9.44
192.8	4.73	4	7.08	387.5	2.35	4	9.34
194.6	4.68	4	6.77	395.6	2.30	4	9.78
196.0	4.65	5	7.25	400.7	2.28	5	9.44
202.3	4.51	4	7.53	410.4	2.22	5	9.41
203.9	4.47	5	7.41	435.0	2.09	5	9.57
207.2	4.40	5	7.64	436.6	2.09	2	9.15
209.3	4.36	4	7.58	449.1	2.03	2	9.34
214.2	4.25	4	7.74	457.0	1.99	3	9.67
215.2	4.24	1	7.69	459.3	1.98	1	9.19
218.5	4.17	*	7.64	461.2	1.98	2	9.57
220.4	4.14	5	8.06	464.3	1.96	1	8.89
227.5	4.01	8	8.18	473.9	1.92	1	8.66
228.0	4.00	*	7.88	479.4	1.90	4	9.25
231.2	3.94	6	8.21	485.6	1.88	1	8.47
233.5	3.90	7	8.20	487.0	1.87	1	8.55
238.5	3.82	5	8.23	492.0	1.85	3	8.28
241.5	3.77	*	7.85	507.4	1.80	3	9.15
243.0	3.75	*	8.15	518.2	1.76	1	7.99
246.2	3.70	6	8.59	525.2	1.74	3	8.47
247.6	3.68	3	8.55	548.8	1.66	2	7.12
248.6	3.67	3	8.49	558.5	1.63	1	7.10
251.5	3.62	*	8.32	575.0	1.58	(Ionization limit)	
256.3	3.56	*	8.51				

Errors in the cell length may arise from a bowing and a thinning of the plastic windows and also from the angular divergence of the beam. The bowing makes the path length longer than that determined from the cell dimensions and increases the attenuation at a given pressure. On the other hand, a reduction in the window thickness would result in a decrease in the attenuation by the windows. A plot of $\ln(I(o)/I(p))$ versus p, which curves concave upwards would indicate that the effect of the window bulge predominates over that of increased transmission due to thinner windows. Similarly (in the absence of second-order radiation), a curve which is concave downward would imply that the effect of the thinning of the plastic windows predominates. How-ever, the graph in Fig. 2 shows that a plot of this kind does result in a straight line and hence over the range of pressures involved no window effect can be detected.

A direct measurement of the change in x as a function of p, indicated that at the highest value of p used in this experiment (15 Torr) the percentage change in x was 3%. A calculation based on the known absorption coefficient of zapon shows that for the range in pressures involved, the increase in transmission arising from a decrease in window thickness is negligible. Thus, errors arising from distortions of the window are within the experimental error.

The increase in path length brought about by the angular divergence of the beam (6° and 0.5°, respec-

FIG. 3. A plot of the cross section as a function of wavelength. The energy range is sufficiently large so that the K, L_1, and $L_{2,3}$ discontinuities are visible. The results of earlier investigations in the vicinity of the three edges is also included for comparison. Range in fluctuations is represented by a vertical bar in the case of GM measurements.
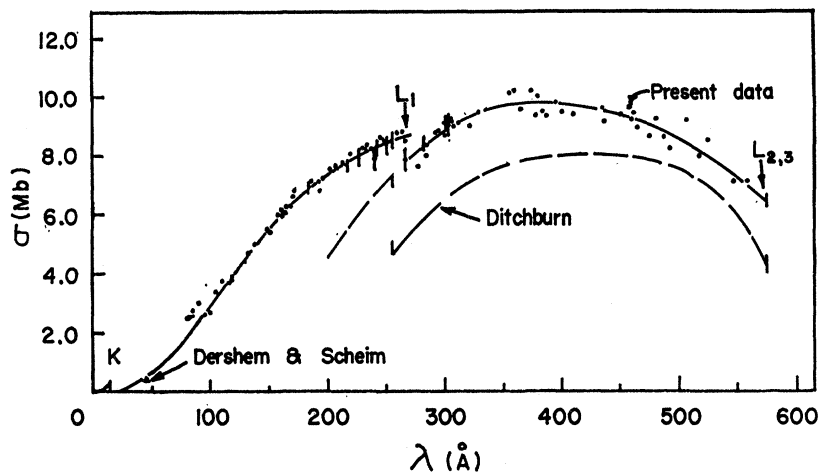
tively, for the grazing and normal incidence spectrograph) was computed to be of the order of 1%. From an over-all consideration of the arguments presented, the systematic error in the result is no greater than 5%. In addition, we assign a random error of ±5% due to the scatter of photometric and counting rate data.

IV. DISCUSSION OF RESULTS

A. Comparison with Earlier Investigations

Figure 3 shows the present determination of the cross section as a function of the incident wavelength. For comparison, earlier values given by Ditchburn[2] are also presented. A curve drawn through the present measurements is extended to include previous data[13-15] at higher photon energies. The interpolation was carried out by fitting the observations at short wavelengths to a relation of the form $\sigma = A\lambda^\alpha$ and extending the plot so as to join the present measurements. The outcome of this procedure is shown in Fig. 4.

At the $L_{2,3}$ threshold (575 Å) the experimental cross section σ has a value of 6.3 Mb and rises to a maximum of 10.0 Mb at 375 Å. The cross section then decreases rapidly as one proceeds to the L_1 edge at about 261 Å where $\sigma = 7.8$ Mb. The jump at the edge is (0.7±0.4) Mb. Towards shorter wavelengths, down to about 90 Å, σ is inversely proportional to the energy. Below 90 Å, the slope of the σ versus λ curve increases smoothly and σ becomes proportional to $\lambda^{2.6}$.

Although the absorption curve shown in Fig. 3 has essentially the same shape as that presented by Ditchburn, the present values of σ are higher by 15%. Both Po Lee and Weissler, and Ditchburn filled their spectrographs with the gas to be studied while in the present work the gas was confined to a small cell. Baker et al.,[5] who also used the cell technique in measuring the cross

section of He, also report values which are higher than the corresponding results of Po Lee and Weissler,[16] and Axelrod et al.[17]

B. Comparison with Theory

The theoretical predictions of Seaton,[18] Cooper,[19] and McGuire[20] are presented in Fig. 5, along with the present data indicated as dots. In comparing theory with experiment we offer the following comments. Seaton
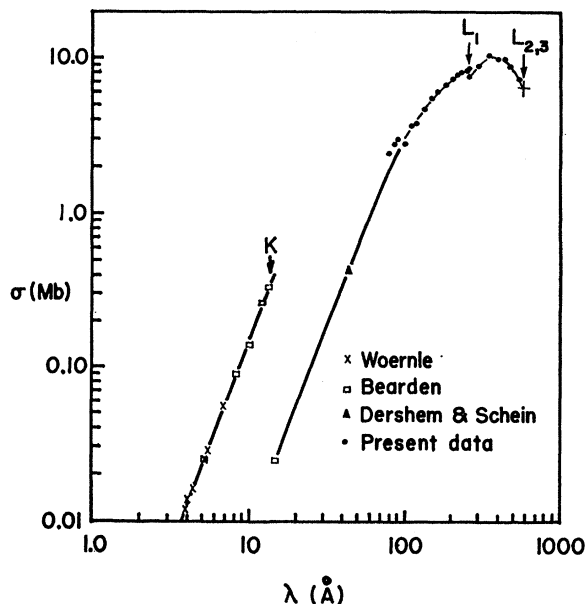

FIG. 4. A plot of the photoionization cross section of neon which shows the manner in which the absorption curve deduced from the present data was interpolated to fit previous measurements at shorter wavelengths.

[13] A. J. Bearden, Bull. Am. Phys. Soc. 8, 312 (1963); and (private communication).

[14] B. Woernle, Ann. Physik 5, 475 (1930).

[15] E. Dershem and M. Schein, Phys. Rev. 37, 1238 (1931).

[16] Po Lee and G. L. Weissler, Phys. Rev. 99, 540 (1955).

[17] N. Axelrod and M. P. Givens, Phys. Rev. 115, 97 (1959).

[18] M. J. Seaton, Proc. Phys. Soc. (London) A67, 927 (1954).

[19] J. W. Cooper, Phys. Rev. 128, 681 (1962).

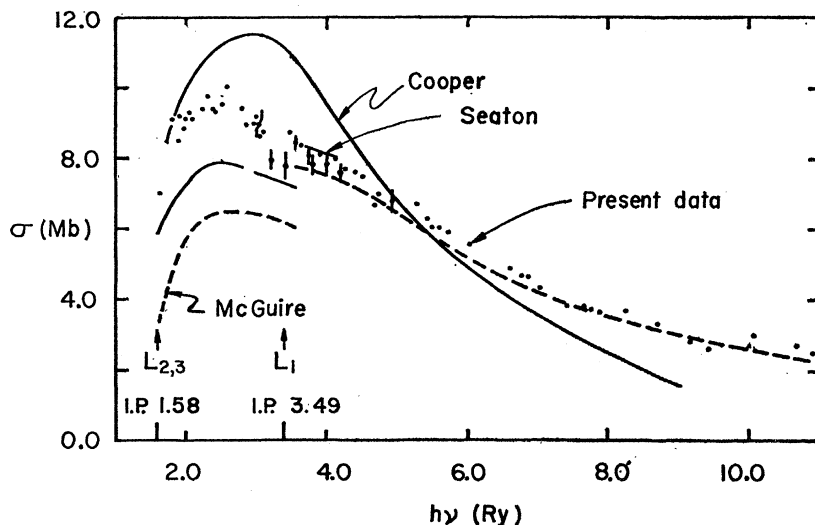[20] E. J. McGuire, Bull. Am. Phys. Soc. 8, 75 (1963); and (private communication).

FIG. 5. The present experimental values of the cross section (plotted as dots) are compared with the results of several theoretical calculations.

and Cooper have approached the problem from a purely theoretical point of view, while the calculation of McGuire is a semiempirical one which utilizes the quantum defect method. The calculated values of σ do not agree but the shapes of the absorption curves are similar to those found by experiment.

In the energy range between the $L_{2,3}$ and the L_1 edges, the experimental cross section falls almost exactly between the results of Seaton and Cooper. McGuire's calculations involve approximations which are valid for photon energies several rydbergs in excess of the photoionization energy. His predictions are in good agreement at energies above the L_1 edge but are too low at smaller energies.

The position of the maximum (see Fig. 5) as predicted by Seaton coincides almost exactly with the experimental value. The corresponding predictions by McGuire and Cooper fall at energies which are higher by 0.2 and 0.4 Ry, respectively. The maximum in σ occurs when the overlap between the bound-state wave function and the continuum wave function is greatest. If the maximum in the calculated cross section occurs at an energy higher than the experimental value, the implication is that the first maximum of the continuum wave function is too far from the core, i.e., the potential is not sufficiently attractive. An examination of Seaton's results leads one to conclude that the outgoing electron moves in the potential of the ion rather than that of the atom. On the other hand, better agreement is expected from McGuire's treatment. In this instance the asymptotic form of the free-electron wave functions are computed using extrapolated experimental values of the quantum defect.

C. The Critical Absorption Edges

An examination of the plots in Figs. 3 and 5 shows a discontinuity centered at about 261 ± 5 Å or 3.49 ± 0.07 Ry. We propose to identify this break with the location

of the L_1 edge. As a first approximation, we may compute the energy required to remove a $2s$ electron from known energy levels[21] in the spectra of Ne I and Ne II. The removal of a $2p$ electron from the neutral Ne atom requires 1.58 Ry. We assume that $(2s-2p)$ energy separation suffers only a slight change as we pass from the neutral to the singly ionized atom. From the known term values arising from the $2s^22p^5$ and the $2s2p^6$ configurations in Ne II the $(L_1-L_{2,3})$ energy difference is 1.98 Ry. Hence the energy required to ionize the $2s$ subshell in the neutral atom is $(1.98+1.58)$ or 3.56 Ry which corresponds to a wavelength of 256 Å. The experimentally observed value is not in conflict with this prediction. A detailed calculation[22] of the change in the $(2s-2p)$ interval as one passes from F I to F⁻ justifies the above assumption that the $(2s-2p)$ interval changes only by a few eV. Previous investigations[1,2] place the L_1 edge between 271 and 247 Å.

In Table II below we summarize additional information relevant to the ionization energy (in Ry) of $1s$, $2s$, and $2p$ electrons in neon.

Cooper's[19] calculations of the ionization energy and those of Worsley[24] are included for comparison. The value of the K absorption limit was obtained from the work of Moore and Chalkin.[25]

The present measurements yield a value of (0.7 ± 0.4) Mb for the jump at the L_1 edge. This is to be compared with the value of 2.6 Mb inferred from previous experi-

[21] C. E. Moore, *Atomic Energy Levels* (U. S. Government Printing Office, Washington, D. C., 1949), Vol. 1.

[22] A self-consistent field calculation (Ref. 23) of $(2s-2p)$ level separation in F I and in F⁻ gives 0.8423 and 0.8956 atomic units, respectively. Consequently, the $(2s-2p)$ separation in F I is 1.45 eV smaller than that in F⁻. Thus, it is reasonable to expect that the prediction of the L_1 edge on the basis of the $(2s-2p)$ separation in the spectrum of Ne II will yield a value which is a few eV smaller than the corresponding separation in Ne I.

[23] L. C. Allen, J. Chem. Phys. **34**, 1156 (1961).

[24] B. H. Worsley, Can. J. Phys. **36**, 289 (1958).

[25] H. R. Moore and F. C. Chalkin, Proc. Phys. Soc. (London) **A68**, 717 (1955).

mental work.[2] Calculations of Seaton and McGuire yield about 1.0 and 2.0 Mb, respectively. Cooper does not compute the $2s$ to continuum cross section, so that his results do not give the magnitude of the L_1 discontinuity.

Recently, Madden and Codling[26] have presented evidence for the existence of transitions from the ground state $^1S_0$ to $^1P_1^0$ states $(2s^2 2p^6 \rightarrow 2s2p^6np)$ in the absorption spectrum of neon. We fail to observe these lines since our source consisted of discrete radiations.

The $^1P_1^0$ states lie above the first ionization limit at 21.56 eV and below the second limit at 48.5 eV corresponding to the removal of one $2s$ electron. Hence there is a possibility of autoionization, that is, the excited atom may become ionized in the $2p$ shell, the excess energy being carried away by a second electron. This nonradiative Auger process competes with radiative transitions from the np states and tends to shorten the mean lifetime of the np states, thus contributing to their widths. The bound $^1P_1^0$ states approach the second ionization limit at 48.5 eV as $n \rightarrow \infty$. Hence, as one approaches the L_1 discontinuity from the low-energy side, one may expect a diffuseness near the onset of the L_1 discontinuity. Moreover, under the appropriate physical conditions, an Auger process may lead to a nonradiative de-ionization of the $2s$ shell and thereby contribute to the width of the L_1 edge.

An examination of the absorption curve reveals the presence of a discontinuity at the expected spectral position. However, owing to the scatter of data it is not feasible to decide unambiguously whether the edge is sharp (less than 0.05 eV) or somewhat diffuse (greater than 0.5 eV). Experimentally, one can set an upper limit of 2.0 eV to the width of the L_1 edge.

D. Oscillator Strength and Sum Rules

Excepting helium,[5,27] neon is the only other rare gas whose photoionization cross section has been studied over a photon energy range of 10 Ry above the threshold. A knowledge of the cross section over a large interval (by measurement or by reasonable interpolation) makes it possible to compute various moments of the oscillator strength distribution after making an estimate of the bound-bound transitions.

The oscillator strength of a dipole transition from the ground state g of an atom to the excited state n is defined by

$$f_{gn} = \tfrac{1}{3}(E_g - E_n)|\langle g| \sum_{i=1}^{N} \mathbf{r}_i |n\rangle|^2, \tag{2}$$

where E_g and E_n, expressed in rydbergs, are the binding energies of the atom in the ground and excited states,

[26] R. Madden and K. Codling, Phys. Rev. Letters **10**, 516 (1963).

[27] J. F. Lowry, thesis, Cornell University (to be published).

TABLE II. The ionization energy (in Ry) of the $1s$, $2s$, and $2p$ electrons in neon. The first column lists approximate energies as computed from atomic energy states. The last column contains the best experimental information. The results of two different theoretical calculations are also given for comparison.

Electron	Atomic energy levels[a]	Theoretical Cooper[b]	Theoretical Worsley[c]	Experimental
$2p$	1.583	1.705	1.705	1.583[d]
$2s$	3.561	3.364	3.866	3.49
$1s$		59.91	65.55	64.13[e]

[a] See Ref. 23.   [c] See Ref. 24.   [e] See Ref. 25.
[b] See Ref. 19.   [d] See Ref. 1.

respectively, and where

$$\langle g| \sum_{i=1}^{N} \mathbf{r}_i |n\rangle = \int \psi_g^* \sum_{i=1}^{N} \mathbf{r}_i \psi_n d\tau \tag{3}$$

is the matrix element associated with the transition. In (3), $\mathbf{r}_i$ is the position vector in units of the Bohr radius of the ith electron, and ψ_g and ψ_n denote the wave functions of the ground and excited states.

The oscillator strength for transitions into the continuum is found by integration of the differential oscillator strength $df/d\epsilon$, which is proportional to the cross section $\sigma(\epsilon)$, as given by the relation

$$\frac{df}{d\epsilon} = \frac{mc}{2\pi^2 e^2 \hbar} \sigma(\epsilon) = K\sigma(\epsilon), \tag{4}$$

where ϵ is the kinetic energy of the ejected electron and the proportionality constant K has the value 0.12387 $\times 10^{19}$ cm^{-2} Ry^{-1}, if the energy is in rydbergs and the remaining constants are expressed in cgs units.

Physically, the oscillator strength is related to a number of observable quantities such as the index of refraction, polarizability, and the diamagnetic susceptibility. The oscillator strengths satisfy a number of sum rules, two of which will be stated here without proof.[28-30] The most important and general of the sum rules is the Thomas-Reiche-Kuhn (hereafter referred to as TRK) rule which is expressed by

$$\sum_n f_{gn} + \int_0^\infty \frac{df}{d\epsilon} d\epsilon = N, \tag{5}$$

where N is the total number of electrons in the atom. A second sum rule which is related to the polarizability α has the form

$$\sum_n f_{gn}(E_g - E_n)^{-2} + \int_0^\infty E^{-2} \frac{df}{d\epsilon} d\epsilon = \frac{\alpha}{4}. \tag{6}$$

[28] For the proofs and derivations of the various sum rules the reader is referred to the treatises by Bethe and Salpeter (Ref. 29) and by Levinger (Ref. 30).

[29] H. A. Bethe and E. E. Salpeter, *Quantum Mechanics of One- and Two-Electron Atoms* (Springer-Verlag, Berlin, 1957).

[30] J. S. Levinger, *Nuclear Photodisintegration* (Oxford University Press, London, 1960).

In relations (5) and (6), E is the energy of the photon defined by $E = hc/\lambda = \epsilon + E_g$, and the integrations are carried out over the states of the continuum while the summations are over the discrete states. For the purpose of evaluation Eqs. (5) and (6) may also be expressed in terms of the wavelength λ. The transformations yield

$$\sum_n f_{gn} + Khc \int_0^{\lambda_0} (\sigma(\lambda)/\lambda^2) d\lambda = N \qquad (7)$$

and

$$4 \sum_n f_{gn}(E_g - E_n)^{-2} + 4K/hc \int_0^{\lambda_0} \sigma(\lambda) d\lambda = \alpha. \qquad (8)$$

For neon, $N = 10$ and this prediction of the TRK sum rule was verified by a numerical integration of σ up to 13 Ry. Above this energy, σ was expressed as a power law and the integration was carried out directly. The result, for transitions into the continuum was found to be 10.2 ± 0.4. The limits given to this result include only random fluctuations, not systematic errors. From Cooper's[19] computations it was estimated that the $2p$ to nd and $2p$ to ns transitions contribute the value 0.3 to the sum. The value of 0.1 was taken as the estimated contribution to the sum by the $2s$ to $2p$ transitions, while the contribution coming from the $1s$ to the np transitions were considered negligible. If we combine the contribution of 0.4 due to the discrete transitions, with the value of 10.2 derived from experiment, the TRK rule gives 10.6 ± 0.4, in excellent agreement with the predicted value of 10. As far as it is known, this is the first time that such a successful confirmation of the TRK sum rule has been obtained.

To verify the sum rule given in (8) σ was plotted as a function of λ and integrated as before. The result of the integration over the continuum was (0.535 ± 0.030) a_0^3 ($a_0 =$ Bohr radius). With the aid of Cooper's[19] value of the oscillator strength for the $2p$ to nd and $2p$ to ns transitions and known term values, it was estimated that the contribution by the discrete transitions from $2p$ subshell amounted to 0.161 a_0^3. The contribution to the sum by discrete transitions from the $2s$ subshell was estimated to be 0.030 a_0^3. Hence the polarizability computed from the sum rule in Eq. (8) is found to be $\alpha = 4 \times 0.726$ $a_0^3 = (0.430 \pm 0.020) \times 10^{-24}$ cm^3. From measurements of the refractive index, Cuthbertson and

Cuthbertson[31] obtained the value $\alpha = 0.398 \times 10^{-24}$ cm^3. There is good agreement between the result of an independent experiment on the measurement of the polarizability and that calculated from the present determination of the cross section. This is significant, because the presence of the E^{-2} term in the integrand of Eq. (6) emphasizes the long-wavelength region.

E. Conclusion

We wish to restate certain features of this investigation. First, the reported values of the cross section represent absolute values whose errors (systematic and random) are at most 5% over the spectral range involved. Such precision has resulted in part from the development of windows transparent to soft x rays. In turn this development allowed the gas under study to be confined to cell and led to reliable measurements of the gas pressure and temperature. Secondly, for the first time, the attenuation has been determined at many wavelengths by the use of a GM counter, developed specifically for this spectral region. The outcome of such determinations was in good agreement with photometric measurements of the attenuation. Thirdly, the range of measurements was extended to ten rydbergs above the photoionization threshold. As a consequence, the results could be joined with measurements made at higher energies by other investigators. Finally, with the exception of helium, neon is the only other gas whose photoionization cross section is known over a large energy range with sufficient precision. This information, in conjunction with estimates of discrete oscillator strengths, has led to the first successful evaluation of the TRK sum rule.

---

[31] C. Cuthbertson and M. Cuthbertson, Proc. Roy. Soc. (London) A84, 13 (1911).